



Published in final edited form as:

Circulation. 2014 March 11; 129(10): 1139–1151. doi:10.1161/CIRCULATIONAHA.113.002416.

HDAC Inhibition Blunts Ischemia/Reperfusion Injury by Inducing Cardiomyocyte Autophagy

Min Xie, MD, PhD¹, Yongli Kong, MD¹, Wei Tan, MD¹, Herman May, BS¹, Pavan K. Battiprolu, PhD¹, Zully Pedrozo, PhD¹, Zhao Wang, PhD¹, Cyndi Morales, BS¹, Xiang Luo, MD¹, Geoffrey Cho, MD¹, Nan Jiang, MS¹, Michael E. Jessen, MD², John J. Warner, MD¹, Sergio Lavandero, PhD^{1,3}, Thomas G. Gillette, PhD¹, Aslan T. Turer, MD¹, and Joseph A. Hill, MD, PhD^{1,4}

¹Dept of Internal Medicine (Cardiology), University of Texas Southwestern Medical Center, Dallas, TX

²Dept of Cardiovascular and Thoracic Surgery, University of Texas Southwestern Medical Center, Dallas, TX

³Centro Estudios Moleculares de la Célula, Facultad de Ciencias Químicas y Farmacéuticas & Facultad de Medicina, Universidad de Chile, Santiago, Chile

⁴Dept of Molecular Biology, University of Texas Southwestern Medical Center, Dallas, TX

Abstract

Background—Reperfusion accounts for a substantial fraction of the myocardial injury occurring with ischemic heart disease. Yet, no standard therapies are available targeting reperfusion injury. Here, we tested the hypothesis that SAHA, a histone deacetylase (HDAC) inhibitor FDA-approved for cancer treatment, will blunt reperfusion injury.

Methods and Results—Twenty-one rabbits were randomized into 3 groups: a) vehicle control, b) SAHA pretreatment (one day prior and at surgery), and c) SAHA treatment at the time of reperfusion only. Each arm was subjected to ischemia/reperfusion surgery (I/R, 30min coronary ligation, 24h reperfusion). Additionally cultured neonatal and adult rat ventricular cardiomyocytes were subjected to simulated I/R (sI/R) to probe mechanism. SAHA reduced infarct (those reduction inhibitor, SAHA, infarct size in a large animal model, even when delivered in the clinically relevant context of reperfusion. The cardioprotective effects of SAHA during I/R occur, at least in part, through induction of autophagic flux. assayed in both rabbit myocardium and in mice harboring an RFP-GFP-LC3 transgene. In cultured myocytes subjected to sI/R, SAHA pretreatment reduced cell death by 40%. This reduction in cell death correlated with increased autophagic activity in SAHA-treated cells. RNAi-mediated knockdown of ATG7 and ATG5, essential autophagy proteins, abolished SAHA's cardioprotective effects.

Conclusions—The FDS-approved anti-cancer HDAC inhibitor, SAHA, reduces myocardial infarct size in a large animal model, even when delivered in the clinically relevant context of reperfusion. The cardioprotective effects of SAHA during I/R occur, at least in part, through induction of autophagic flux.

Copyright © 2014 American Heart Association, Inc. All rights reserved.

Address for Correspondence: Joseph A. Hill, MD, PhD Division of Cardiology University of Texas Southwestern Medical Center NB11.200, 6000 Harry Hines Boulevard Dallas, TX 75390-8573 Tel: 214-648-1400 Fax: 214-648-1450 joseph.hill@utsouthwestern.edu.

Conflict of Interest Disclosures: None.

Keywords

ischemia; reperfusion injury; neuroprotection; autophagy; HDAC

Introduction

Five million Americans suffer from chronic heart failure, the final common pathway of many forms of heart disease and the most common discharge diagnosis in Medicare for several years running¹. This syndrome carries a mortality of approximately 50% at 5 years, and its incidence and prevalence are expanding rapidly around the globe². Coronary artery disease is the leading cause of heart failure with reduced ejection fraction (HFrEF)³. In the context of myocardial infarction (MI), the extent of myocardial damage correlates directly with the extent of LV remodeling³. Indeed, significant advances in anti-platelet and anti-thrombotic agents, novel devices (e.g. drug-eluting stents), and an abiding focus on time to reperfusion have proven critical for decreasing infarct size and preserving systolic function⁴. Nevertheless, data from the VALIANT study demonstrate that with modern percutaneous coronary intervention, the overall mortality rate reaches 25% three years following ST segment elevation MI (STEMI)⁵. Thus, there appears to be a ceiling on our ability to mitigate infarct size by restoration of coronary artery patency alone.

Often, ischemia is followed by reperfusion, when the infarct-related artery recanalizes, either spontaneously or in response to therapeutic intervention. This event, which restores oxygen and nutrients to the injured tissue, triggers a complex cascade of events and a second wave of injury⁶. Indeed, reperfusion injury is a major contributor to infarct size, approaching 50% of total injury burden⁷. To address this problem, several small clinical trials have evaluated therapies such as ischemic post-conditioning, cyclosporine, and hypothermia, and some have demonstrated protective effects⁸. However, as yet no standard therapy exists, and an effective and clinically feasible therapy to mitigate reperfusion injury is sorely needed.

Many proteins are regulated by reversible acetylation of ϵ -amino groups on lysine residues. Appreciated first in the case of histone proteins, where acetylation leads to chromatin relaxation and access of transcriptional activators to DNA⁹, this widespread post-translational modification occurs on numerous proteins beyond just histones. Reversible protein acetylation is governed by enzymes that attach (histone acetyltransferases, HATs) or remove (histone deacetylases, HDACs) acetyl groups. In the case of the latter, small molecule inhibitors of HDACs are currently being tested for a variety of oncological indications. In mammalian cells, 18 HDACs have been described, grouped into four classes¹⁰. Gene deletion and over-expression studies have revealed important functions of several of these enzymes in pathological cardiac remodeling, including ventricular hypertrophy, apoptosis, necrosis, metabolism, contractility, and fibrosis^{11, 12}.

A series of preclinical studies, including those from our laboratory, have demonstrated potent cardioprotective benefits of HDAC inhibitors in murine models of myocardial stress, including I/R¹³⁻¹⁶. Trichostatin A (TSA), an HDAC inhibitor specific to class I and II HDACs, reduces myocardial infarct size up to 50%^{15, 16}. TSA or another HDAC inhibitor, Scriptaid, reduced one hour after the ischemic insult still reduced infarct size to an extent similar to pretreatment¹⁶. These exciting results suggest that HDAC inhibition may be suitable to treat patients presenting with myocardial infarction at the time of percutaneous coronary intervention in the cardiac catheterization laboratory. However, recent evidence has unveiled surprisingly large differences in disease mechanisms in murine models of disease relative to the human case¹⁷. These facts, coupled with the fact that an HDAC inhibitor which is structurally similar to TSA, SAHA (suberoylanilide hydroxamic acid;

vorinostat) is FDA-approved for treatment of cutaneous T-cell lymphoma, led us to test SAHA's efficacy in a large animal model of I/R.

Materials and Methods

Mouse model of I/R

8-12 week old C57BL6 wild-type mice were anesthetized with 2.4% isoflurane and placed in a supine position on a heating pad (37°C). Animals were intubated with a 19G stump needle and ventilated with room air using a MiniVent mouse ventilator (Hugo Sachs Elektronik; stroke volume 250 μ L, respiratory rate 210 breaths per minute). Following left thoracotomy between the fourth and fifth ribs, the LAD (Left Anterior Descending coronary artery) was visualized under a microscope and ligated using a 6-0 prolene suture. Regional ischemia was confirmed by visual inspection under a dissecting microscope (Leica) of discoloration of the occluded distal myocardium. For I/R, the ligation was released after 45 minutes of ischemia and the tissue allowed to re-perfuse as confirmed by visual inspection. Sham-operated animals underwent the same procedure without occlusion of the LAD. All procedures were approved by the UT Southwestern IACUC.

Rabbit I/R protocol

Rabbits (6-8 lb male New Zealand White rabbits; Provance) were anesthetized with ketamine (40 mg/kg) plus xylazine (5 mg/kg). The animal was intubated and placed on mechanical ventilation. Fur was removed over the site of the incision and disinfected with surgical iodine. The animal was draped with sterile drapes. A warming light and Bair Hugger® were used to maintain body temperature within a range of 35-37°C. Thoracotomy was performed via the fourth intercostal space. The circumflex artery was located and ligated with suture material (4-0 silk) attached to a non-traumatic needle. This snare was tightened to occlude the artery for 30 minutes (ischemia). The snare was then released, and reperfusion was confirmed visually. The retractor was removed and the lung re-inflated. The chest was then closed with 2-0 PDS suture, and the muscles and skin are closed by layer using 3-0 PDS absorbable suture and tissue adhesive, respectively. The animals were observed during recovery from anesthesia. After surgery, rabbits were treated with buprenorphine 0.05 mg/kg and, if necessary, once again the next morning for analgesia. Pain was assessed by signs of discomfort, lethargy, or anorexia. 24 hours from reperfusion, rabbits were re-anesthetized with ketamine (40 mg/kg) plus xylazine (5 mg/kg). The deeply anesthetized animals were then sacrificed with 20-60mg/kg of sodium pentobarbital. The heart was then excised with the ascending aorta preserved for cannulation. All procedures were approved by the UT Southwestern IACUC.

For protein and imaging studies, ischemia was imposed for 30 minutes followed by 2 hours of reperfusion. After sacrifice, the rabbit hearts were perfused with a 5% solution of phthalo blue dye (Heucotech, Fairless Hill, PA) in normal saline to delineate the area at risk and remote zone. One set of animals was used for protein study (four animals per group). The heart was divided into three tissue zones: infarct zone (2-3 mm inside the line of blue dye), remote zone (2-3 mm outside the line of blue dye), and border zone (the remainder of the left ventricle after removal of infarct and remote zones). Each zone of tissue was minced into small pieces, divided equally into three tubes, and flash frozen for subsequent Western blot analysis. Another set of animals (three per group) was used for EM (electron microscopy) and TUNEL (Terminal deoxynucleotidyl transferase dUTP Nick End Labeling) analyses.

TTC staining

At the time of anesthesia and prior to sacrifice, rabbits were given heparin 1000 unit/kg for anticoagulation to ensure that the dye perfused well. The heart was excised and perfused with PBS solution (5 mL) through an aortic cannula (fitted with a suture to close the aorta around the cannula). To delineate the occluded-reperfused coronary vascular bed, the coronary artery was then tied at the site of the previous occlusion, and the aortic root was perfused with a 5% solution of phthalo blue dye in normal saline (5 mL over 5 min). Using this procedure, the portion of the LV supplied by the previously occluded coronary artery (area at risk, AAR) was identified by the absence of blue dye, whereas the rest of the LV was stained dark blue.

To harvest samples for molecular biological analysis, hearts were cut in half and then 5-6 small samples (2mm × 2mm) were harvested using scissors and forceps. Next, atrial and right ventricular tissues were excised. Then, the LV tissue was frozen and cut into 7 slices. To delineate infarcted from viable myocardium, the heart slices were incubated with 1% solution of 2,3,5-triphenyltetrazolium chloride (TTC) in phosphate buffer (pH 7.4, 37°C) at 37°C (50 mL per heart) for 40 min. The heart slices were then fixed in 10% neutral buffered formaldehyde and 24 hour later weighed and photographed digitally. With this procedure, the non-ischemic portion of the LV was stained dark blue, viable tissue within the region at risk was stained bright red, and infarcted tissue was white or light yellow. The images were analyzed using ImageJ, and from these measurements infarct size was calculated as a percentage of the region at risk using a weight-based method.

Measurement of autophagic flux in mice

Mice harboring a RFP-GFP-LC3 transgene driven by a CAG promoter were generated. Mice were randomized into three groups. One group received vehicle, DMSO (dimethyl sulfoxide), as control, one group received the SAHA pretreatment protocol (50 mg/kg SQ x4), and the last group received the SAHA reperfusion protocol (100mg/kg SQ x1). The mice were subjected to 45 min of ischemia and 2 hour reperfusion. GFP and RFP signals were detected in frozen sections by confocal microscopy.

Measurement of plasma SAHA concentration

One hundred microliters of plasma were mixed with 200µL of acetonitrile (containing 0.15% formic acid, 300 ng/mL benzylbenzamide as internal standard). The samples were vortexed 15 sec, incubated at room temperature for 10 min and spun twice at 13,200 rpm in a standard microcentrifuge. The supernatant was then analyzed by LC/MS/MS. Buffer A: Water + 0.1% formic acid; Buffer B: MeOH + 0.1% formic acid; flow rate 1.5 mL/min; column Agilent C18 XDB column, 5 micron packing 50 × 4.6 mm size ; 0-1 min 95% A, 1-1.5 min gradient to 95% B; 1.5-2.5 min 100% B, 2.5-2.6 min gradient to 95% A; 2.6-3.5 min 95% A; IS N-benzylbenzamide (transition 212.1 to 91.1); Compound transition 265.1 to 232.021.

Primary culture of neonatal rat ventricular myocytes (NRVM)

Briefly, left ventricles from 1- to 2-day-old Sprague-Daley rats were collected and digested with collagenase. The resulting cell suspension was pre-plated to clear fibroblasts. We then plated collagenase. The resulting cell suspension was pre-plated to clear fibroblasts. We then plated the cells at a density of 1250 cells per 1 mm² in medium containing 10% FBS (fetal bovine serum) µmol/L bromodeoxyuridine (BrdU). Typical cultures were notable for >95% cardiomyocytes.

Isolation and culture of primary adult rat ventricular myocytes (ARVMs)

ARVMs were isolated from hearts of male adult Sprague Dawley rats (250-350g). Rats were anesthetized with pentobarbital (i.p.), hearts were removed, washed with Gerard buffer [0.19 mM NaH₂PO₄, 1.01 mM Na₂HPO₄, 10 mM HEPES, 128 mM NaCl, 4 mM KCl, 1.4 mM MgSO₄, 5.5 mM glucose, 2 mM pyruvic acid (pH 7.4)] and retroperfused (5 mL/min) with 2 mM CaCl₂-containing Gerard buffer for 5 min, followed by 2 mM EGTA-containing Gerard buffer for 1 min, and finally with 0.12% (wt/vol) collagenase A (Roche)-containing Gerard buffer (digestion solution) for 30 min. Digested hearts were mechanically shattered in 20 mL digestion solution, incubated at 37°C with constant agitation for 10 min and supernatants centrifuged at 500 rpm for 30 sec. Remaining tissue was further digested with 20 mL digestion solution. Pellets containing cardiac myocytes were washed in Gerard buffer and then resuspended in plating medium (DMEM supplemented with 5% FBS, 1xITS, 10 mM 2,3-butanedione monoxime, and 100 U/mL penicillin-streptomycin). After calcium was reintroduced, cardiac myocytes were plated at a final density of $1.0 \times 10^3/\text{mm}^2$ on laminin pre-coated culture dishes or coverslips. Culture medium (DMEM supplemented with 1xITS, 10 mM 2,3-butanedione monoxime and 100 U/mL penicillin-streptomycin) was replaced 4 hours later.

Simulated I/R in cultured cells and cell death assay

For simulated ischemia/reperfusion (sI/R) NRVM studies, ischemia was imposed by a buffer exchange to ischemia-mimetic solution (in mM: 20 deoxyglucose, 125 NaCl, 8 KCl, 1.2 KH₂PO₄, 1.25 MgSO₄, 1.2 CaCl₂, 6.25 NaHCO₃, 5 sodium lactate, 20 HEPES, pH 6.6) and placing the culture plates within a humidified gas chamber equilibrated with 95% N₂, 5% CO₂. After 2-5 h of simulated ischemia, reperfusion was initiated by buffer exchange to normoxic NRVM culture medium with 10% FBS and incubation in 95% room air, 5% CO₂. Controls incubated in normoxic NRVM culture medium with 10% FBS were prepared in parallel for each condition. Cell death was detected using the CytoTox 96 Non-Radioactive Cytotoxicity Assay (G1781, Promega).

For ARVMs, 2 μ M SAHA or DMSO was added 12h before sI/R in the control and I2 groups (pre-treatment). 2 μ M SAHA or DMSO was added at reperfusion for a total of 2h treatment in the I2R2 group (cells were treated with sI/R of two hours ischemia and two hours reperfusion). LC3 Western blots were performed to assay autophagic flux. ARVM cell death was evaluated by microscopy. Each group was studied in triplicate, and two representative views were examined for each sample. With four repeats, each group comprised a total 24 readings.

Reagents

Antibodies for immunoblotting were as follows: rabbit anti-LC3 was prepared in our lab based on synthetic peptides. GAPDH antibody was from Santa Cruz Biotechnology (Santa Cruz, CA), ATG7 antibody was from Anaspec (54231), respectively. ATG5 antibody was from Abcam (ab108327) and cleaved caspase-3 antibody was from Cell Signaling (#9664). TSA was purchased from Biomol (Plymouth Meeting, PA). SAHA and Bafilomycin A were purchased from LC Laboratory.

siRNA knockdown

NRVMs were isolated and seeded at a density of 1.2 million/well in a 6-well dish. 24 hours after plating, cardiomyocytes were incubated with siRNA negative control (Neg, SIC001), siRNAs targeting ATG7 (top two rankings against rat, SASI_Rn01_00050326 and SASI_Rn01_00050327), or siRNAs targeting ATG5 (SASI_Rn01_00094887 and SASI_Rn01_00094888), each from Sigma and used according to the manufacturer's

recommended protocols. Briefly, siRNAs were reconstituted into a 40 mM stock solution. 3 μ L of the siRNA stock and 3 μ L of RNAiMax transfectant were mixed together in 1 mL Optima medium. Cardiomyocytes were incubated with the RNAiMax for 6 hours, followed by addition of 1 mL of culture medium containing 20% serum. 24 hours after the siRNA incubation, the cardiomyocytes were treated with SAHA at 2mM (overnight). Then, the cells were subjected to ischemia (5 hours) and reperfusion (1.5 hours) for cell death assay.

Electron microscopy (EM)

Hearts were retrograde perfused using PBS and 2% glutaraldehyde in 0.1 M cacodylate buffer. Post-fixation occurred in 2% osmium tetroxide in 0.1 M cacodylate buffer and 1% aqueous uranyl acetate, each for 1 hour. An ascending series of ethanol washes (50%, 70%, 90%, 100%) was performed, followed by transitioning to propylene oxide and then a 1:1 mixture of propylene oxide and EMBED 812 (Electron Microscopy Sciences). The tissue was incubated in EMBED for 1 hour, then placed in a 70°C oven to polymerize. Sections (75–80 nm) were cut using a Leica ultramicrotome and a Diatome diamond knife, collected on 200-mesh copper grids and poststained in 5% uranyl acetate in ethanol (10 minutes) and Reynold's lead citrate (5 minutes). A JEOL 1200 EX transmission electron microscope, operating at 40–120 kV and equipped with a digital camera, was used to image the sections.

Adenoviral infection of cultured cardiomyocytes

NRVMs were plated as above on cover slips. 24 hours after plating, cells were infected with adenovirus expressing GFP-LC3 (MOI 10). After treating the cells with SAHA or DMSO overnight, they were fixed with 4% PFA (paraformaldehyde) and examined by confocal fluorescence microscopy.

Immunoblot analysis

Protein lysates were separated by SDS/PAGE, transferred to Hybond-C nitrocellulose membrane (HYBOND-ECL Nitrocellulose), and subjected to immunoblot analysis.

TUNEL Staining

TUNEL staining was performed using the In Situ Cell Death Detection kit (Roche) according to the manufacturer's instructions. PI (propidium iodide) staining was performed to visualize nuclei after TUNEL reaction and the percentage of TUNEL positive nuclei was quantified using ImageJ software. To overlay the striated muscle fiber with TUNEL signals, a differential interference contrast microscopy (DIC) image was taken at 400X magnification.

Echocardiography

Rabbit echocardiograms were performed on anesthetized rabbits (ketamine 40 mg/kg plus xylazine 5 mg/kg) using an Acuson Sequoia C512 (software Sequoia 9.51) system and a 15L8 Acuson linear probe. A short axis view of the left ventricle at the level of the papillary muscles was obtained, and M-mode recordings were obtained from this view. Left ventricular internal diameter at end-diastole (LVIDd) and end-systole (LVIDs) were measured from M-mode recordings. Fractional shortening was calculated as $(LVIDd - LVIDs)/LVIDd$ (%).

Mouse echocardiograms were performed on conscious, gently restrained mice using a Vevo 2100 system and an 18-MHz linear probe. A short axis view of the left ventricle at the level of the papillary muscles was obtained, and M-mode recordings were obtained from this view. Fractional shortening was calculated using the same approach as in rabbit.

Statistical methods

Averaged data are reported as mean \pm SEM. Data were analyzed with the unpaired Student *t* test for 2 independent groups, paired *t* test for dependent data, and the 1-way ANOVA followed by the Tukey post-hoc test for pairwise comparisons. Studies with repeat measures were analyzed using repeated measures ANOVA. For all statistical tests, a *p* value <0.05 was considered statistically significant, and all tests were two-tailed. For animal studies (both mouse and rabbit data), normality tests were assessed via the Shapiro–Wilk and Anderson–Darling statistics. As normality was confirmed (**Suppl. Table 1**), results are presented from parametric statistics. In the case of non-normality, non-parametric tests have been used (Mann-Whitney U test for two group comparisons and the Kruskal-Wallis test for 3 groups followed by Dunn's test to correct for multiple comparisons). To be most stringent, all animal data and statistical comparisons were verified using non-parametric methods regardless of passing normality tests (**Suppl. Table 2**). All statistical analyses were performed using GraphPad Prism (version 6.01) software.

Results

TSA and SAHA reduce infarct and preserve systolic function in mouse I/R

TSA has been previously reported to reduce infarct size around 50% in an *ex vivo* Langendoff and *in vivo* mouse model of I/R^{15, 16}. To verify and extend these findings, we treated C57BL6 mice with TSA 1 mg/kg IP one day before *in vivo* I/R (ischemia 45 min and reperfusion 24 hours). Infarct size and area at risk for infarction were determined by TTC staining (**Fig. 1a**). TSA reduced infarct size, normalized to area at risk (IF/AAR), by around 50%, a result comparable to earlier studies (**Fig. 1b**)^{15, 16}. There was no significant difference in the area at risk between the two groups (**Fig. 1c**), confirming that the surgical injury was equivalent between treatment groups. Similar findings emerged when infarct size was normalized to left ventricle weight (IF/LV), which was reduced by around 50% (**Fig. 1d**).

Echocardiography was performed in mice injected daily with TSA (1 day, 3 days, 1 week, 2 weeks) following surgery to evaluate ventricular size and systolic function. These data revealed significant TSA-dependent protection (**Figs. 1b, 1d**), which persisted through the entire two week observation period (**Fig. 1e**).

We next set out to determine whether SAHA, an FDA-approved hydroxamic acid-based compound structurally similar to TSA with similar HDAC isoform specificity, afforded similar benefit. SAHA has an IC_{50} 30-50 times greater than that of TSA and different pharmacokinetics^{18, 19}. We therefore tested two doses of SAHA, 30 mg/kg and 50 mg/kg, which are within the range of the doses used in cancer studies²⁰⁻²². We followed a pretreatment protocol, in which mice received SAHA subcutaneously (SQ) q12h one day before surgery (2 doses), a third dose one-half hour before surgery, and a fourth dose at the time of reperfusion. Throughout, the surgeon, echocardiographer, and TTC staining interpreter were blinded to treatment group assignments. SAHA (50 mg/kg) reduced infarct size by around 45% ($p < 0.05$) (**Fig. 1f, 1g**). Lower dose SAHA (30 mg/kg) manifested a trend toward reduced infarct size ($\approx 20\%$) which failed to achieve statistical significance. We observed no difference in area at risk across all the groups (**Fig. 1h**). Echocardiographic analysis demonstrated that SAHA treatment (50 mg/kg) partially preserved systolic function after I/R (%FS increased from $40 \pm 2\%$ to $50 \pm 3\%$, $p < 0.05$, $n = 6-7$) (**Fig. 1i**). In aggregate, these data establish that SAHA is functionally similar to TSA in its ability to blunt I/R damage in mice.

SAHA reduces infarct size and preserves systolic function in rabbit I/R

In some instances, the human response to disease-related stress differs substantially from that observed in murine models¹⁷, emphasizing the critical importance of testing in large animals before moving to humans. With a vision toward translating our findings to the clinical context, we tested the effects of SAHA in I/R injury in a large animal model. Given that rabbits metabolize SAHA approximately three-fold faster than mice¹⁹, we tested a range of doses to identify an optimal dose (**Suppl. Fig. 1a**). We also devoted considerable effort to carefully mapping the coronary anatomy in the rabbit, which is known to be highly variable²³, in order to achieve a stable area at risk (**Suppl. Fig. 1b**).

Rabbits were randomized among 3 treatment arms (**Fig. 2**). In one arm (pretreatment), rabbits received SAHA 150 mg/kg subcutaneously (SQ) q12h one day before surgery (2 doses), a third dose one-half hour before surgery, and a fourth dose at the time of reperfusion. In the second treatment arm (reperfusion-only), animals received two doses of vehicle (DMSO) prior to surgery and a single dose of SAHA at 300 mg/kg at the time of reperfusion. Finally the third arm (control) received vehicle injections for all four injection times. Animals were randomized to one of three treatment groups by a single investigator, who was the only investigator aware of treatment assignment.

Both the pretreatment and reperfusion-only treatment arms manifested significantly reduced infarct size normalized to area at risk ($28\pm 4\%$, $34\pm 4\%$ respectively) as compared with the control arm ($50\pm 2\%$) (**Figs. 3a, 3b**). There were no differences in area at risk across the three groups, confirming that the surgical procedures were similar (**Fig. 3c**). Infarct size normalized to left ventricle weight also manifested significant reduction ($p<0.05$, $n=7$) in both the pretreatment ($8.1\pm 2\%$) and reperfusion-only ($10.4\pm 1\%$) treatment arms as compared with control ($15\pm 1\%$) (**Fig. 3d**).

Echocardiography was performed and percent fractional shortening (%FS) was measured as an index of cardiac function, both before and after I/R. Baseline echocardiographic analysis of ventricular function revealed no significant differences among treatment groups prior to I/R. Measurements obtained 24 hours after surgery demonstrated a decrease in %FS from $33.5\pm 0.6\%$ to $19\pm 0.5\%$ ($p<0.001$, $n=7$) in the control group (**Figs. 3e, 3f**). This decrease in systolic function was mitigated by SAHA treatment, regardless of whether the drug was administered prior to surgery (%FS declined from $34.7\pm 0.5\%$ to $26\pm 1\%$, $p<0.001$, $n=7$) or exclusively at reperfusion (%FS declined from $33.7\pm 0.6\%$ to $27\pm 1\%$, $p<0.001$, $n=7$, **Fig. 3f**).

Similar protective effects afforded by SAHA were observed in the preliminary experiments we performed to optimize the surgical I/R intervention. When this data set was combined with our blinded/randomized preclinical trial, the statistical significance was even more robust (**Suppl. Figs. 1c, 1d** non-randomized, **Suppl. Figs. 1e-1h** combined). These data provide strong evidence that SAHA blunts I/R-induced declines in infarct size and systolic function by $\approx 50\%$ (**Fig. 3g**).

SAHA serum concentrations comparable to human

As noted, the rate of SAHA metabolism in rabbit is substantially faster than in humans¹⁹. To establish a correlation between the SAHA serum concentrations effective in blunting I/R injury in rabbits with levels achievable clinically in humans, we measured SAHA serum levels. To determine the cumulative exposure to drug, we calculated the Area Under the Curve (AUC) by measuring plasma SAHA concentrations at 15, 30, 60, 120, 240, 360, 480 min and 24 hour after a single dose of SAHA (300 mg/kg SQ). In eight rabbits, the C_{max} was $3.3\pm 0.4\ \mu\text{M}$, time to peak concentration (T_{max}) was 1.0 ± 0.5 hour, the 8-hour AUC was $12.7\pm 1.3\ \mu\text{M}\cdot\text{hr}$, and the 24-hour AUC was $20.6\pm 2.0\ \mu\text{M}\cdot\text{hr}$ (**Fig. 4**). In comparison, human

subjects with T cell lymphoma receiving a high dose SAHA regimen (800 mg PO daily) achieved a C_{max} of $1.7 \pm 0.7 \mu\text{M}$ and a median T_{max} of 2.1 (0.5-6 hours), with a mean AUC of $8.6 \pm 5.7 \mu\text{M}\cdot\text{hr}$. In other words, the pharmacokinetics and serum concentrations of SAHA achieved in our rabbit study, with drug delivered SQ, exceed those seen in humans receiving PO dosing⁸. In one phase 1 clinical trial, patients received various doses of SAHA intravenously: 75, 150, 300, 600, and 900 600 mg/m²/day²⁴. By comparison with these data, the SAHA drug exposure in rabbit falls within the moderate dose range (300 to 600 mg/m²/day) (Table 1)²⁴. These data suggest that the drug exposure we achieved in rabbit is comparable to that observed in human subjects receiving either two PO doses of SAHA or an IV dose of SAHA.

SAHA increases autophagy in the infarct border zone

Autophagy is an evolutionarily conserved cellular process in which the cell isolates, degrades, and recycles portions of the cytoplasm, including damaged organelles. Alterations in autophagic activity have been linked to a variety of pathological conditions and can be either adaptive or maladaptive, depending on the context²⁵. Autophagy has been recognized to be involved in reperfusion injury²⁶. By replenishing energy stores during ischemia and removing damaged mitochondria, autophagy can act to protect the cardiomyocyte from damage that might lead to cell death²⁶. SAHA has been shown to increase autophagy in cancer cells²⁷. In order to assess the role of autophagy in the cardioprotective effect of SAHA in I/R, we randomized 16 rabbits and treated them with either SAHA (300 mg/kg SQ at reperfusion) or vehicle (DMSO). The animals were sacrificed two hours after reperfusion, and the hearts isolated and analyzed as three distinct zones: a remote zone distant from the ischemic area, an infarct zone within the center of the area perfused by the ligated artery, and a border zone that surrounded the site of infarction (Fig. 5a).

Autophagy was evaluated initially by Western blot detection of the autophagosome-associated lipidated isoform of LC3 (LC3-II). LC3-II levels, reflective of autophagosome-associated lipidated isoform of LC3 (LC3-II). LC3-II levels, reflective of autophagosome abundance, were similar in the infarct, remote, and border zones of hearts of the vehicle-treated group. By contrast, significant increases in LC3-II levels were detected in the border zone of hearts in the SAHA treatment arm as compared with the infarct or remote zones (Fig. 5b). Autophagosome accumulation in the infarct border zone of SAHA-treated hearts was verified by electron microscopy (EM) (Fig. 5c). Also, consistent with a decrease in infarct size, apoptosis (measured by TUNEL assay and cleaved caspase-3) was also decreased within the infarct border zone of SAHA-treated rabbits (Suppl. Fig. 2 and 3).

Autophagy is a dynamic process of flux. As such, increased steady state levels of autophagosomes can signify either an increase of autophagy, a block in downstream lysosomal processing of these autophagosomes, or both. We therefore assayed autophagic flux, or autophagosome biogenesis, maturation, and lysosomal degradation, using mice that we engineered to harbor a RFP-GFP-LC3 transgene driven by a CAG promoter. Yellow puncta, reflective of combined GFP and RFP fluorescence, mark autophagosomes, whereas red puncta (RFP only) mark autolysosomes whose acidic pH quenches GFP fluorescence. Under conditions where flux is blocked, an increase in yellow signal is observed with little increase in the red signal. Mice were subjected to 45 min of ischemia and 2 hour reperfusion, and GFP and RFP signals were detected in frozen sections. In the infarct border zone of SAHA-treated mice (using either the pretreatment protocol; 50 mg/kg SQ x4 or the reperfusion-only protocol; 100mg/kg SQ once at the time of reperfusion), both GFP/RFP and RFP signals were significantly increased, indicating increased incorporation of LC3 into both autophagosomes and autolysosomes (Fig. 5d). These data, then, suggest that the accumulation of autophagosomes observed in the infarct border zone of SAHA-treated

rabbits derives from a *bona fide* increase in autophagic flux. SAHA's cardioprotective effects are dependent on autophagic flux.

SAHA's cardioprotective effects are dependent on autophagic flux

To examine whether increases in autophagic flux contribute to the cardioprotective effects of SAHA, we turned to an *in vitro* assay of simulated ischemia/reperfusion (sI/R). Neonatal rat ventricular myocytes (NRVM) were treated with SAHA or vehicle overnight and then subjected to five hours of simulated ischemia followed by 1.5 hours of simulated reperfusion. We first examined cell death by measuring LDH levels in the culture medium. Exposure of NRVM's to sI/R resulted in a greater than four-fold increase in cell death (**Fig. 6a**). SAHA treatment, however, elicited a significant decrease in sI/R-induced cell death. These results are consistent with the *in vivo* cardioprotective properties of SAHA (**Fig. 6a**).

To examine autophagic activation preceding cell death, NRVMs were exposed to sI/R (2 hour ischemia only, I2h; or 2 hour ischemia and 2 hour reperfusion, I2hR2h) in the presence/absence of SAHA. Of note, we selected 2 hour ischemia instead of 5 hour ischemia in the cell death assays in order to focus on early molecular processes preceding cell death. Steady-state levels of LC3-II were slightly decreased during both the ischemic and reperfusion stages of injury. These decreases correlated with a decrease in autophagic flux as demonstrated by decreased levels of LC3-II observed after blocking lysosomal activity with Bafilomycin A (Baf A). In the absence of Baf A, LC3-II levels were similar in both vehicle and SAHA treatment groups; however lysosomal inhibition by Baf A uncovered a dramatic increase in autophagic flux induced by SAHA, as evidenced by significant accumulation of LC3II (**Fig. 6b**). We confirmed this activation of autophagic flux by SAHA using an LC3-GFP adenovirus. NRVM's treated with SAHA manifested a noticeable increase in LC3-GFP puncta formation as compared to the DMSO control (**Fig. 6c**). This increase was similar to that observed with the established autophagy inducer rapamycin (**Fig. 6c**).

Induction of autophagic flux by SAHA treatment both before sI/R and at reperfusion was also observed in ARVMs. Microscopic methods were used to detect ARVM cell death based on distinct morphological changes, an approach employed previously to quantify I/R-induced ARVM cell death^{28, 29}. SAHA treatment at the time of reperfusion significantly attenuated sI/R-induced cell death suggesting that this cardioprotective effect is not specific to neonatal cells (**Suppl. Figs. 4 and 5**).

Having established that SAHA induces autophagic flux and decreases sI/R-induced cell death, we next examined whether this increased autophagy was required for the protection we observed. The effect of SAHA on cell survival was measured in the presence of siRNA targeting each of two essential autophagy proteins, ATG7 or ATG5. Again, SAHA treatment protected NRVMs from sI/R-induced cell death. However, knockdown of either ATG7 or ATG5 abolished the protective effect of SAHA (**Fig. 6d and Suppl. Fig. 6a**). In each case, two sequence-independent siRNAs were tested to confirm specificity. Additionally, RNAi-dependent depletion of either ATG7 or ATG5 had no effect on the levels of the other protein. (**Fig. 6e and Suppl. Fig. 6b**). These data, then, point to a critical requirement of autophagic flux in the cardioprotective actions of SAHA.

To mimic *in vitro* conditions of reperfusion-only treatment, we tested the effect of SAHA when added at the time of reperfusion during simulated I/R. Consistent with our findings with SAHA pretreatment, SAHA added at the time of simulated reperfusion induced autophagic flux in NRVM (**Fig. 7a**) and increased NRVM survival (**Fig. 7b**). This reperfusion-only cardioprotection was also dependent on autophagy, as knockdown of ATG7 resulted in a loss of the survival benefit of SAHA treatment (**Fig. 7b**).

In our prior studies using a model of chronic pressure-overload hypertrophy, we have shown that long-term treatment (7 days) with TSA led to a reduction in autophagic flux³⁰. At face value, this seems to contradict SAHA-induced increases in autophagic flux seen here. However, autophagic flux was, in fact, down-regulated in cultured NRVM treated with TSA in serum-free medium for 48 hours³⁰. Given this, we reasoned that this apparent discrepancy may derive from differences in the conditions and duration of HDAC inhibition employed in our two studies.

To test this directly, NRVM's were treated with TSA or SAHA in the presence/absence of Bafilomycin A, and cells were collected over the course of 3-48 hours post-treatment. Western blot analysis demonstrated an increase in autophagic flux with TSA treatment that peaked at 12 hours and diminished significantly below baseline by 48 hours (**Suppl. Fig. 7**). SAHA treatment manifested a similar pattern (**Suppl. Fig. 7**). Thus, HDAC inhibition appears to elicit a time-dependent biphasic effect on autophagic flux.

Discussion

Ischemia/reperfusion is a major mechanism of injury in many forms of cardiovascular disease. In this setting, both the ischemic and reperfusion phases of the process confer harm to a roughly equivalent extent. Whereas many means of mitigating ischemic injury have emerged, comprising the standard-of-care in patients with coronary artery disease, no standard therapies are presently available to target reperfusion injury.

Recent work has uncovered a significant cardioprotective effect of HDAC inhibition in I/R injury^{15, 16}. These studies, which are remarkably concordant and emerging from independent labs, have relied on mouse models of I/R injury. Further, mechanisms underlying this benefit of HDAC inhibition remain obscure.

Here, we have extended these studies with a preclinical trial in a large animal model. We have employed rigorous methodology mimicking those typical of a clinical trial: pre-specified endpoints and power calculations, randomization, and strict blinding of personnel. With this approach, we have uncovered robust cardioprotective effects of SAHA in rabbits. Further, preservation of contractile performance and the $\approx 40\%$ decreases in infarct size were essentially equivalent when animals were pretreated with drug or when the drug was administered exclusively at the time of reperfusion. Our studies went on to identify an effect of SAHA to promote autophagic flux in cardiomyocytes within the infarct border zone, which was required for its cardioprotective activity. Finally, we demonstrate that SAHA-dependent activation of autophagic flux is required for the benefit.

HDAC inhibition in I/R injury

HDAC inhibition has been shown to blunt pathological remodeling in models of pressure overload^{14, 30}. Given this, HDAC inhibitors have also been tested in another prevalent form of pathological stress, cardiac ischemia³¹. In a rat model of myocardial infarction, the HDAC inhibitors valproic acid and tributyrin reduced cardiomyocyte hypertrophy and collagen deposition in both the remote and border zones of the infarcted left ventricle³². Systolic function was also preserved. Finally, these protective effects were abolished by theophylline, an HDAC activator³².

Two studies tested HDAC inhibitors in murine ischemia/reperfusion (I/R). Using an *ex vivo* Langendorff model, both perfusion of the explanted heart with TSA or treatment of the animal with TSA before surgery reduced infarct size and preserved systolic function¹⁵. TSA-induced p38 activation and acetylation of p38 at lysine residues were posited as underlying mechanisms¹⁵. Another study reported that HDAC activity increased

significantly after cardiac I/R *in vivo*, and HDAC inhibition (TSA, Scriptaid) reduced infarct size and preserved systolic function¹⁵. Another study reported that HDAC activity increased significantly after cardiac I/R *in vivo*, and HDAC inhibition (TSA, Scriptaid) reduced infarct size and preserved systolic function¹⁶. Of note, administration of the HDAC inhibitor one hour after the ischemic insult reduced infarct size to an extent similar to that observed with pretreatment prior to surgical injury¹⁶. This study also reported that HDAC inhibition reduced hypoxia inducible factor-1 levels, diminished vascular permeability, and cell death¹⁶.

In a murine model of myocardial infarction, TSA stimulated c-kit+ cardiac stem cell (CSC) proliferation³³. In c-kit-null mice, TSA's beneficial effects were abolished, and re-introduction of TSA-treated wild-type c-kit+ CSCs into c-kit-null mice restored the beneficial remodeling effects of TSA³³. After exposure to TSA, the abundance of c-kit+ CSC-derived myocytes was significantly increased³³. Together, these findings raise the possibility that HDAC inhibition could be used initially as an infarct-size reducing strategy and subsequently as long-term therapy to blunt post-infarct remodeling by mobilizing cardiac stem cells.

HDAC inhibition in myocardial I/R: translating to the human case

We report here that SAHA confers robust cardioprotection in a large animal model of myocardial I/R. These experiments were conducted in the context of two HDAC inhibitors, namely Zolinza® (vorinostat, structurally similar to TSA) and Istodax® (romidepsin), having received FDA approval for use in cutaneous T cell lymphoma. Meanwhile, clinical trials with several others are underway in a number of tumor types. Given the pressing clinical need for drugs to treat I/R and the current availability of HDAC inhibitors approved for human use, we turned our attention to consideration of testing in humans.

It should be acknowledged that many agents targeting reperfusion injury have failed in clinical testing; why should SAHA be any different? Examination of those prior trials is instructive, revealing several reasons that could explain the failure⁸. In some cases, strategies tested in preclinical models did not manifest robust cardioprotective benefit. Many were not verified in multiple independent labs. Often, the tested agents were not administered at the time of reperfusion to mimic the clinical context. Many were not tested in a large animal model. In some cases, protocols required of a rigorous clinical trial were not employed⁸. In light of these failings, we have addressed each of these issues with data that are robust, reproducible across independent labs, and concordant across species. Further, benefits seen when the drug is delivered at reperfusion were similar to those seen when the animal is pretreated with drug.

In other words, SAHA fulfills the most stringent requirements for a successful anti-reperfusion injury agent in myocardial infarction patients. HDAC inhibition has been demonstrated in at least three independent labs, including ours, to reduce infarct size robustly (around 50%) in a murine I/R model^{15, 16}. SAHA is available as an FDA-approved anti-cancer HDAC inhibitor with an acceptable safety profile²⁴. In addition, we report here that SAHA reduces infarct size and preserves systolic function after I/R injury, delivered at reperfusion, in a large animal model.

These findings suggest that SAHA has the potential to emerge as an anti-reperfusion injury therapeutic strategy. However, limitations should be acknowledged. Surgical ligation of a disease-free coronary artery is not equivalent to thrombotic occlusion of a diseased vessel in a patient with comorbidities. To address this concern rigorously, a pilot efficacy clinical trial in patients with ischemic heart disease is required.

SAHA's plasma concentration is achievable in human subjects

The metabolism of SAHA in rabbit differs from that in human, being approximately 3-fold more rapid¹⁹. Nevertheless, the C_{max} of SAHA in rabbit is similar to that observed in patients receiving oral therapy, and the 8-hour AUC is only 50% higher than that in humans. We believe that the high 24-hour AUC in rabbit is artificially prolonged, deriving from a depot effect of SQ injection, as the plasma concentration has decreased below therapeutic levels eight hours after injection (around four half-lives)¹⁸. In addition, it is noteworthy that the AUCs measured in patients with cancer were obtained in the context of multiple comorbidities and multiple drug exposures, likely provoking gastrointestinal disturbance, renal dysfunction, and a fasting state¹⁸. Thus, higher C_{max} and AUC might be achievable in STEMI patients, who are typically not fasted when presenting for PCI, using an 800 mg PO dose. Alternatively, two separate doses one hour apart could be administered. In any event, the AUC observed in rabbit is readily achievable in humans exposed to moderate doses delivered IV²⁴.

Another issue is the safety of SAHA in myocardial infarction patients. Most of the side effects of SAHA are reported in patients with end-stage cancer receiving additional chemotherapeutic agents. In patients taking SAHA chronically and on a regular basis (months or years), deep venous thrombosis, leuko- and thrombocytopenia, bone marrow suppression and gastrointestinal side effects have been reported¹⁸. Whereas we do not envision chronic administration, these observations nevertheless highlight the need for careful surveillance for safety.

Effects of HDAC inhibition on autophagic flux and the consequent cardioprotective effects

The adaptive or maladaptive effects of autophagy on cardiac pathology are tightly linked to both the extent of autophagy and the type of stress eliciting the response. Interestingly, there is no consensus regarding whether autophagic flux is increased or impaired during cardiomyocyte reperfusion²⁶. Matsui et al demonstrated a clear decrease in infarct size in a mouse model of *BECN1* haploinsufficiency³⁴. However, recent studies from Ma et al challenge the assumption that *BECN1* haploinsufficiency merely prevents autophagy initiation, suggesting that it may also act to increase autophagic processing³⁵. Ma et al demonstrated that the up-regulation of Beclin observed after reperfusion was coupled with a decline in LAMP2 which resulted in diminished autophagic processing. This decrease was rescued by an increase in LAMP2 or a decrease in Beclin³⁵. Our findings support the latter model. Indeed, our findings are in agreement with a number of studies that suggest that an increase in autophagy during I/R is protective³⁵⁻³⁷. Our data show that SAHA treatment increases autophagy specifically in the border zone of I/R-stressed hearts. This increase in autophagy correlates with protection against I/R cell death *in vivo* and is required for protection by SAHA against cell death in sI/R *in vitro*.

It is interesting that HDAC inhibition increases autophagic flux primarily in the border zone, where active cell death is taking place. One possible explanation is that cardiomyocytes in the ischemic/infarct zone are lethally injured beyond rescue, whereas uninjured cardiomyocytes in the remote zone lack cues driving autophagosome formation. The sublethally stressed cardiomyocytes in the border zone, however, remain viable and subject to either intracellular or extracellular cues that modulate autophagic flux, a response enhanced by HDAC inhibition.

The ability of SAHA to induce autophagy is consistent with findings in cancer cells treated with SAHA, although the end result of autophagic stimulation in cardiomyocyte I/R appears to be cytoprotective and not cytotoxic as in cancer cells^{38, 39}. Mechanistic studies in cancer

reveal that SAHA elicits inhibition of mTOR and the subsequent induction of autophagic flux⁴⁰. Whether this mechanism pertains to cardiomyocytes is currently under investigation.

In contrast to the observations reported here that SAHA induces autophagy on short-term exposure, we have reported previously that chronic HDAC inhibition suppresses autophagy³⁰. Whereas at first glance these findings appear to be contradictory, closer examination is instructive. First, chronic HDAC inhibition in a pressure overload model *in vivo*, or in NRVMs in culture, resulted in reduction of autophagic flux³⁰. Here, we exposed mice or rabbits to SAHA transiently. Second, cultured NRVMs in this report were studied in the presence of serum and with only brief serum-free exposure during ischemia. Indeed, we have collected experimental evidence that differences in drug exposure and experimental model are relevant. Nevertheless, both studies point to an intriguing ability of HDAC inhibition to suppress excess autophagic flux or restore impaired autophagic flux to a zone that is beneficial^{2, 41}.

Other mechanisms underlying SAHA cardioprotection

HDAC inhibition has broad effects on gene expression as well as direct effects on protein activity through promotion of protein hyperacetylation. Additionally, as yet unidentified off-target effects may exist¹¹. It has been reported that SAHA has anti-inflammatory properties^{42, 43}. However, it is doubtful this accounts for the majority of the cardioprotective effects of SAHA, as solely targeting inflammation during reperfusion injury does not substantially limit infarct size⁴⁴. Further, evaluation here of a selected subset of anti-inflammatory mediators did not reveal significant SAHA-dependent changes (data not shown). Also, SAHA has been suggested to promote the proliferation and homing of stem cells^{33, 45}. However, given the short duration of our reperfusion injury studies, it seems unlikely that activation of stem cells plays an important role in SAHA-dependent cardioprotection. Nevertheless, recent studies suggesting that enhanced stem cell activity is critical during the remodeling stage of myocardial infarction open the possibility of benefit from a longer treatment regimen³³. Our data point to increases in autophagic flux as the primary mechanism of SAHA's cardioprotective effects. Indeed, inhibition of autophagy by specific depletion of ATG7 or ATG5 blocked the ability of SAHA to rescue cells during sI/R. Further work is required to define specific mechanisms, including HDAC protein targets that modulate autophagic flux in cardiomyocyte I/R.

Conclusions and perspective

Preservation of systolic function post-MI correlates with improved clinical outcomes⁴⁶. Here, we demonstrate that an FDA-approved HDAC inhibitor, SAHA, reduces myocardial infarct size in a large animal model. Re-activation of I/R-triggered down-regulated autophagy is a major underlying mechanism. Currently, molecular mechanisms underlying SAHA's cardioprotective effects, as well as HDAC-dependent control of cardiomyocyte autophagy, remain unknown. However, we submit that this therapeutic strategy holds promise in addressing the global scourge of ischemic cardiovascular disease.

Supplementary Material

Refer to Web version on PubMed Central for supplementary material.

Acknowledgments

We thank members of the Hill lab for helpful discussions and critique. We also thank Mr. Colby Ayers for critical advice regarding statistical analyses.

Funding Sources: This work was supported by grants from the NIH (HL-080144, HL-0980842, HL-100401), CPRIT (RP110486P3), the AHA DeHaan Foundation (0970518N), and the Fondation Leducq (11CVD04).

References

1. Go AS, Mozaffarian D, Roger VL, Benjamin EJ, Berry JD, Borden WB, Bravata DM, Dai S, Ford ES, Fox CS, Franco S, Fuller-ton HJ, Gillespie C, Hailpern SM, Heit JA, Howard VJ, Huffman MD, Kissela BM, Kittner SJ, Lackland DT, Lichtman JH, Lisabeth LD, Magid D, Marcus GM, Marelli A, Matchar DB, McGuire DK, Mohler ER, Moy CS, Mussolino ME, Nichol G, Paynter NP, Schreiner PJ, Sorlie PD, Stein J, Turan TN, Virani SS, Wong ND, Woo D, Turner MB. Heart disease and stroke statistics--2013 update: A report from the american heart association. *Circulation*. 2013; 127:e6–e245. [PubMed: 23239837]
2. Heidenreich PA, Trogon JG, Khavjou OA, Butler J, Dracup K, Ezekowitz MD, Finkelstein EA, Hong Y, Johnston SC, Khera A, Lloyd-Jones DM, Nelson SA, Nichol G, Orenstein D, Wilson PW, Woo YJ. Forecasting the future of cardiovascular disease in the united states: A policy statement from the american heart association. *Circulation*. 2011; 123:933–944. [PubMed: 21262990]
3. Fraccarollo D, Galuppo P, Bauersachs J. Novel therapeutic approaches to post-infarction remodelling. *Cardiovasc Res*. 2012; 94:293–303.
4. Dorn GW 2nd. Novel pharmacotherapies to abrogate postinfarction ventricular remodeling. *Nat Rev Cardiol*. 2009; 6:283–291. [PubMed: 19352332]
5. Pfeffer MA, McMurray JJ, Velazquez EJ, Rouleau JL, Kober L, Maggioni AP, Solomon SD, Swedberg K, Van de Werf F, White H, Leimberger JD, Henis M, Edwards S, Zelenkofske S, Sellers MA, Califf RM. Valsartan, captopril, or both in myocardial infarction complicated by heart failure, left ventricular dysfunction, or both. *N Engl J Med*. 2003; 349:1893–1906. [PubMed: 14610160]
6. Turer AT, Hill JA. Pathogenesis of myocardial ischemia-reperfusion injury and rationale for therapy. *Am J Cardiol*. 2010; 106:360–368. [PubMed: 20643246]
7. Yellon DM, Hausenloy DJ. Myocardial reperfusion injury. *N Engl J Med*. 2007; 357:1121–1135.
8. Schwartz Longacre L, Kloner RA, Arai AE, Baines CP, Bolli R, Braunwald E, Downey J, Gibbons RJ, Gottlieb RA, Heusch G, Jennings RB, Lefler DJ, Mentzer RM, Murphy E, Ovize M, Ping P, Przyklenk K, Sack MN, Vander Heide RS, Vinten-Johansen J, Yellon DM. New horizons in cardioprotection: Recommendations from the 2010 national heart, lung, and blood institute workshop. *Circulation*. 2011; 124:1172–1179. [PubMed: 21900096]
9. Yang XJ, Seto E. Lysine acetylation: Codified crosstalk with other posttranslational modifications. *Mol Cell*. 2008; 31:449–461. [PubMed: 18722172]
10. Gregoretti IV, Lee YM, Goodson HV. Molecular evolution of the histone deacetylase family: Functional implications of phylogenetic analysis. *J Mol Biol*. 2004; 338:17–31. [PubMed: 15050820]
11. McKinsey TA. Therapeutic potential for hdac inhibitors in the heart. *Annu Rev Pharmacol Toxicol*. 2012; 52:303–319. [PubMed: 21942627]
12. Berry JM, Cao DJ, Rothermel BA, Hill JA. Histone deacetylase inhibition in the treatment of heart disease. *Expert Opin Drug Saf*. 2008; 7:53–67.
13. Antos CL, McKinsey TA, Dreitz M, Hollingsworth LM, Zhang CL, Schreiber K, Rindt H, Gorczyński RJ, Olson EN. Dose-dependent blockade to cardiomyocyte hypertrophy by histone deacetylase inhibitors. *J Biol Chem*. 2003; 278:28930–28937. [PubMed: 12761226]
14. Kong Y, Tannous P, Lu G, Berenji K, Rothermel BA, Olson EN, Hill JA. Suppression of class i and ii histone deacetylases blunts pressure-overload cardiac hypertrophy. *Circulation*. 2006; 113:2579–2588. [PubMed: 16735673]
15. Zhao TC, Cheng G, Zhang LX, Tseng YT, Padbury JF. Inhibition of histone deacetylases triggers pharmacologic preconditioning effects against myocardial ischemic injury. *Cardiovasc Res*. 2007; 76:473–481. [PubMed: 17884027]
16. Granger A, Abdullah I, Huebner F, Stout A, Wang T, Huebner T, Epstein JA, Gruber PJ. Histone deacetylase inhibition reduces myocardial ischemia-reperfusion injury in mice. *FASEB J*. 2008; 22:3549–3560. [PubMed: 18606865]
17. Seok J, Warren HS, Cuenca AG, Mindrinos MN, Baker HV, Xu W, Richards DR, McDonald-Smith GP, Gao H, Hennessy L, Finnerty CC, Lopez CM, Honari S, Moore EE, Minei JP,

- Cuschieri J, Bankey PE, Johnson JL, Sperry J, Nathens AB, Billiar TR, West MA, Jeschke MG, Klein MB, Gamelli RL, Gibran NS, Brownstein BH, Miller-Graziano C, Calvano SE, Mason PH, Cobb JP, Rahme LG, Lowry SF, Maier RV, Moldawer LL, Herndon DN, Davis RW, Xiao W, Tompkins RG. Genomic responses in mouse models poorly mimic human inflammatory diseases. *Proc Natl Acad Sci USA*. 2013; 110:3507–3512. [PubMed: 23401516]
18. Merck Sharp & Dohme Corp. asoMC, Inc.. [october 2012] Physician's prescribing information for zolinza® (vorinostat). via www.Zolinza.Com/vorinostat/zolinza/consumer/prescribing-zolinza/index/jsp
 19. Wise LD, Turner KJ, Kerr JS. Assessment of developmental toxicity of vorinostat, a histone deacetylase inhibitor, in sprague-dawley rats and dutch belted rabbits. *Birth Defects Res B Dev Reprod Toxicol*. 2007; 80:57–68. [PubMed: 17294457]
 20. Kilgore M, Miller CA, Fass DM, Hennig KM, Haggarty SJ, Sweatt JD, Rumbaugh G. Inhibitors of class 1 histone deacetylases reverse contextual memory deficits in a mouse model of alzheimer's disease. *Neuropsychopharmacology*. 2010; 35:870–880. [PubMed: 20010553]
 21. Chen MY, Liao WS, Lu Z, Bornmann WG, Hennessey V, Washington MN, Rosner GL, Yu Y, Ahmed AA, Bast RC Jr. Decitabine and suberoylanilide hydroxamic acid (saha) inhibit growth of ovarian cancer cell lines and xenografts while inducing expression of imprinted tumor suppressor genes, apoptosis, g2/m arrest, and autophagy. *Cancer*. 2011; 117:4424–4438. [PubMed: 21491416]
 22. More SS, Itsara M, Yang X, Geier EG, Tadano MK, Seo Y, Vanbrocklin HF, Weiss WA, Mueller S, Haas-Kogan DA, Dubois SG, Matthey KK, Giacomini KM. Vorinostat increases expression of functional norepinephrine transporter in neuroblastoma in vitro and in vivo model systems. *Clin Cancer Res*. 2011; 17:2339–2349. [PubMed: 21421857]
 23. Podesser B, Wollenek G, Seitelberger R, Siegel H, Wolner E, Firbas W, Tschabitscher M. Epicardial branches of the coronary arteries and their distribution in the rabbit heart: The rabbit heart as a model of regional ischemia. *Anat Rec*. 1997; 247:521–527. [PubMed: 9096792]
 24. Kelly WK, Richon VM, O'Connor O, Curley T, MacGregor-Curtelli B, Tong W, Kiang M, Schwartz L, Richardson S, Rosa E, Drobnjak M, Cordon-Cordo C, Chiao JH, Rifkind R, Marks PA, Scher H. Phase i clinical trial of histone deacetylase inhibitor: Suberoylanilide hydroxamic acid administered intravenously. *Clin Cancer Res*. 2003; 9:3578–3588. [PubMed: 14506144]
 25. Rubinsztein DC, Codogno P, Levine B. Autophagy modulation as a potential therapeutic target for diverse diseases. *Nat Rev Drug Discov*. 2012; 11:709–730.
 26. Przyklenk K, Dong Y, Undyala VV, Whittaker P. Autophagy as a therapeutic target for ischaemia/reperfusion injury? Concepts, controversies, and challenges. *Cardiovasc Res*. 2012; 94:197–205. [PubMed: 22215722]
 27. Lopez G, Torres K, Lev D. Autophagy blockade enhances hdac inhibitors' pro-apoptotic effects: Potential implications for the treatment of a therapeutic-resistant malignancy. *Autophagy*. 2011; 7:440–441. [PubMed: 21224727]
 28. Shahzad T, Kasseckert SA, Iraqi W, Johnson V, Schulz R, Schluter KD, Dorr O, Parahuleva M, Hamm C, Ladilov Y, Abdallah Y. Mechanisms involved in postconditioning protection of cardiomyocytes against acute reperfusion injury. *J Mol Cell Cardiol*. 2013; 58:209–216. [PubMed: 23328483]
 29. Kang PM, Haunstetter A, Aoki H, Usheva A, Izumo S. Morphological and molecular characterization of adult cardiomyocyte apoptosis during hypoxia and reoxygenation. *Circ Res*. 2000; 87:118–125. [PubMed: 10903995]
 30. Cao DJ, Wang ZV, Battiprolu PK, Jiang N, Morales CR, Kong Y, Rothermel BA, Gillette TG, Hill JA. Histone deacetylase (hdac) inhibitors attenuate cardiac hypertrophy by suppressing autophagy. *Proc Natl Acad Sci U S A*. 2011; 108:4123–4128. [PubMed: 21367693]
 31. Xie M, Hill JA. Hdac-dependent ventricular remodeling. *Trends Cardiovasc Med*. 2013; 23:229–235. [PubMed: 23499301]
 32. Lee TM, Lin MS, Chang NC. Inhibition of histone deacetylase on ventricular remodeling in infarcted rats. *Am J Physiol Heart Circ Physiol*. 2007; 293:H968–977. [PubMed: 17400721]
 33. Zhang L, Chen B, Zhao Y, Dubielecka PM, Wei L, Qin GJ, Chin YE, Wang Y, Zhao TC. Inhibition of histone deacetylase-induced myocardial repair is mediated by c-kit in infarcted hearts. *J Biol Chem*. 2012; 287:39338–39348. [PubMed: 23024362]

34. Matsui Y, Takagi H, Qu X, Abdellatif M, Sakoda H, Asano T, Levine B, Sadoshima J. Distinct roles of autophagy in the heart during ischemia and reperfusion: Roles of amp-activated protein kinase and beclin 1 in mediating autophagy. *Circ Res.* 2007; 100:914–922. [PubMed: 17332429]
35. Ma X, Liu H, Foyil SR, Godar RJ, Weinheimer CJ, Hill JA, Diwan A. Impaired autophagosome clearance contributes to cardiomyocyte death in ischemia/reperfusion injury. *Circulation.* 2012; 125:3170–3181. [PubMed: 22592897]
36. Buss SJ, Muenz S, Riffel JH, Malekar P, Hagenmueller M, Weiss CS, Bea F, Bekeredjian R, Schinke-Braun M, Izumo S, Katus HA, Hardt SE. Beneficial effects of mammalian target of rapamycin inhibition on left ventricular remodeling after myocardial infarction. *J Am Coll Cardiol.* 2009; 54:2435–2446. [PubMed: 20082935]
37. Sala-Mercado JA, Wider J, Undyala VV, Jahania S, Yoo W, Mentzer RM Jr, Gottlieb RA, Przyklenk K. Profound cardioprotection with chloramphenicol succinate in the swine model of myocardial ischemia-reperfusion injury. *Circulation.* 2010; 122:S179–184. [PubMed: 20837911]
38. Li J, Liu R, Lei Y, Wang K, Lau QC, Xie N, Zhou S, Nie C, Chen L, Wei Y, Huang C. Proteomic analysis revealed association of aberrant ros signaling with suberoylanilide hydroxamic acid-induced autophagy in jurkat t-leukemia cells. *Autophagy.* 2010; 6:711–724. [PubMed: 20543569]
39. Thomas S, Thurn KT, Bicaku E, Marchion DC, Munster PN. Addition of a histone deacetylase inhibitor redirects tamoxifen-treated breast cancer cells into apoptosis, which is opposed by the induction of autophagy. *Breast Cancer Res Treat.* 2011; 130:437–447. [PubMed: 21298336]
40. Banreti A, Sass M, Graba Y. The emerging role of acetylation in the regulation of autophagy. *Autophagy.* 2013; 9:819–829. [PubMed: 23466676]
41. Masiero E, Agatea L, Mammucari C, Blaauw B, Loro E, Komatsu M, Metzger D, Reggiani C, Schiaffino S, Sandri M. Autophagy is required to maintain muscle mass. *CellMetab.* 2009; 10:507–515.
42. Halili MA, Andrews MR, Labzin LI, Schroder K, Matthias G, Cao C, Lovelace E, Reid RC, Le GT, Hume DA, Irvine KM, Matthias P, Fairlie DP, Sweet MJ. Differential effects of selective hdac inhibitors on macrophage inflammatory responses to the toll-like receptor 4 agonist lps. *J Leukoc Biol.* 2010; 87:1103–1114. [PubMed: 20200406]
43. Lin HS, Hu CY, Chan HY, Liew YY, Huang HP, Lepescheux L, Bastianelli E, Baron R, Rawadi G, Clement-Lacroix P. Anti-rheumatic activities of histone deacetylase (hdac) inhibitors in vivo in collagen-induced arthritis in rodents. *Br J Pharmacol.* 2007; 150:862–872. [PubMed: 17325656]
44. Timmers L, Pasterkamp G, de Hoog VC, Arslan F, Appelman Y, de Kleijn DP. The innate immune response in reperfused myocardium. *CardiovascRes.* 2012; 94:276–283.
45. Burba I, Colombo GI, Staszewsky LI, De Simone M, Devanna P, Nanni S, Avitabile D, Molla F, Cosentino S, Russo I, De Angelis N, Soldo A, Biondi A, Gambini E, Gaetano C, Farsetti A, Pompilio G, Latini R, Capogrossi MC, Pesce M. Histone deacetylase inhibition enhances self renewal and cardioprotection by human cord blood-derived cd34 cells. *PloS One.* 2011; 6:e22158. [PubMed: 21789227]
46. Otterstad JE, Ford I. The effect of carvedilol in patients with impaired left ventricular systolic function following an acute myocardial infarction. How do the treatment effects on total mortality and recurrent myocardial infarction in capricorn compare with previous beta-blocker trials? *Eur J Heart Fail.* 2002; 4:501–506. [PubMed: 12167391]

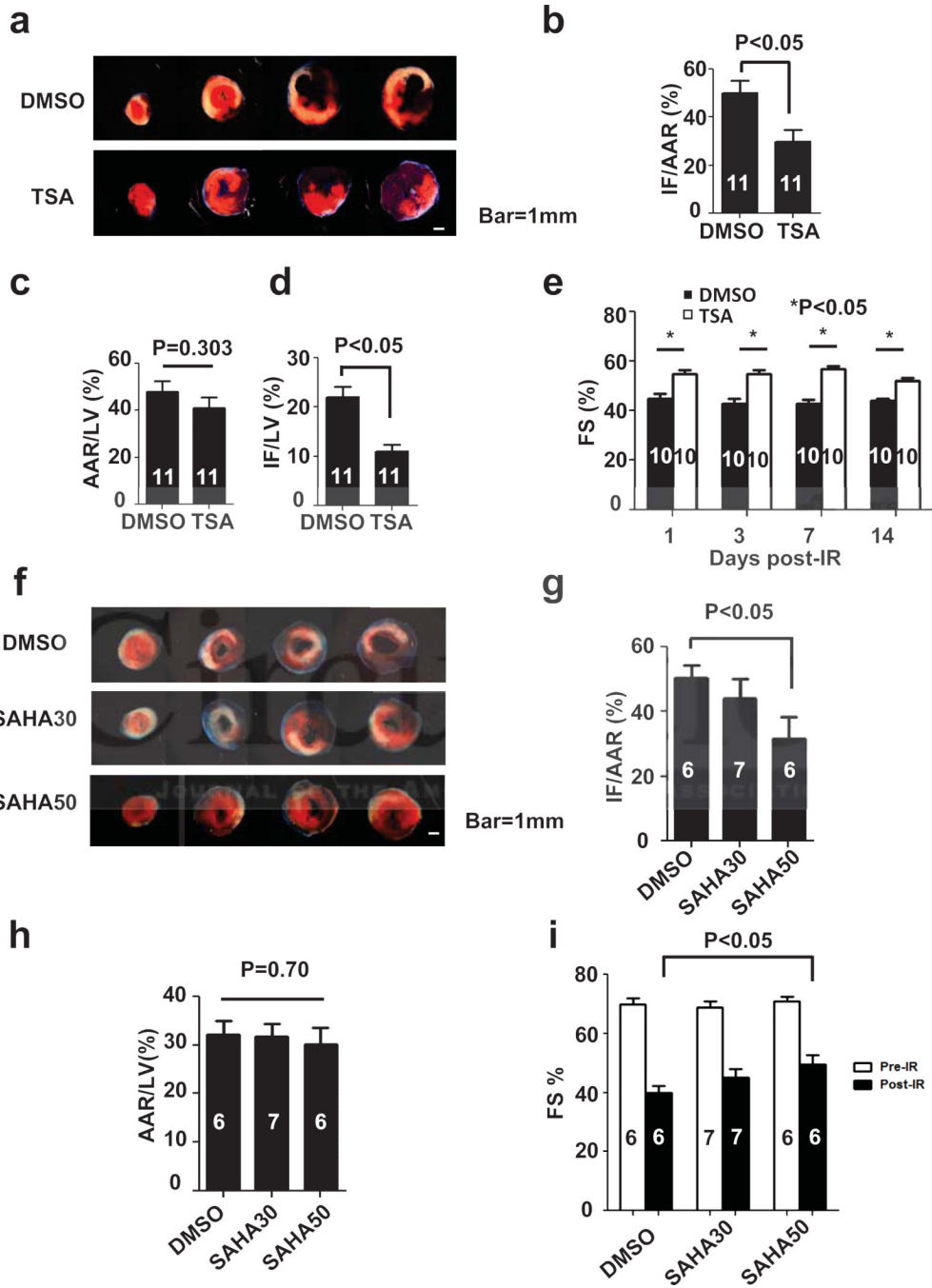
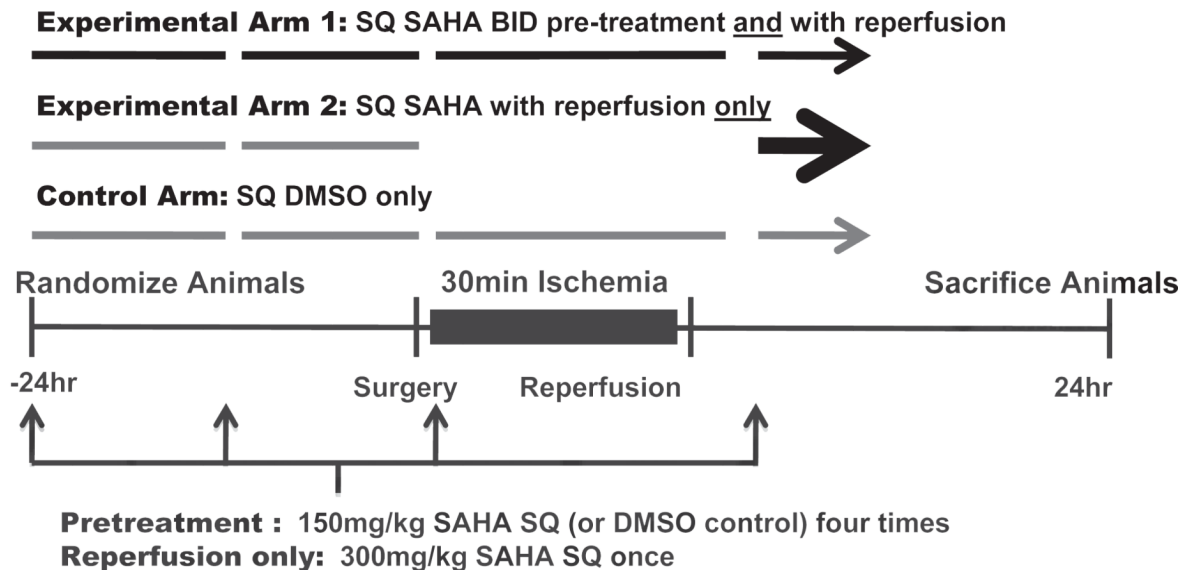


Figure 1. TSA and SAHA reduce infarct size and preserve systolic function in mouse I/R. **a.** Representative TTC staining of TSA and DMSO pretreatment groups after I/R (45 min/24 hour). White: Infarct, Red: AAR, Blue: Remote. **b.** TSA reduced infarct (IF) size normalized to area at risk (AAR) (n=11, p<0.05) as determined by TTC staining after I/R. **c.** There were no significant differences in AAR among groups. **d.** TSA reduced IF normalized to left ventricle weight (LV) (n=11, p<0.05). **e.** TSA daily injection for up to total 14 days treatment improved systolic function measured as %FS after I/R (n =10, p<0.05). **f.** Representative TTC staining of SAHA and DMSO pretreatment groups after I/R (45 min/24

hour) **g.** SAHA pretreatment before I/R (50 mg/kg, SAHA50) reduced IF/AAR significantly (n=6-7, p<0.05). SAHA at a lower dose (30 mg/kg, SAHA30) did not achieve statistical significance. **h.** There were no significant differences in AAR among groups. **i.** SAHA treatment partially preserved %FS measured by echocardiography after I/R (n=6-7, p<0.05).

**Figure 2.**

Experimental design testing SAHA's cardioprotective effects. Experimental Arm 1: The pretreatment group received SAHA 150 mg/kg subcutaneously (SQ) q12h one day before the surgery, one dose a half hour before surgery, and one dose at the time of reperfusion. Experimental Arm 2: The reperfusion-only group received two doses of vehicle (DMSO) one day before surgery and one dose of SAHA (300 mg/kg) at the time of reperfusion. Control Arm: The control group received only four doses of DMSO, the vehicle used for SAHA.

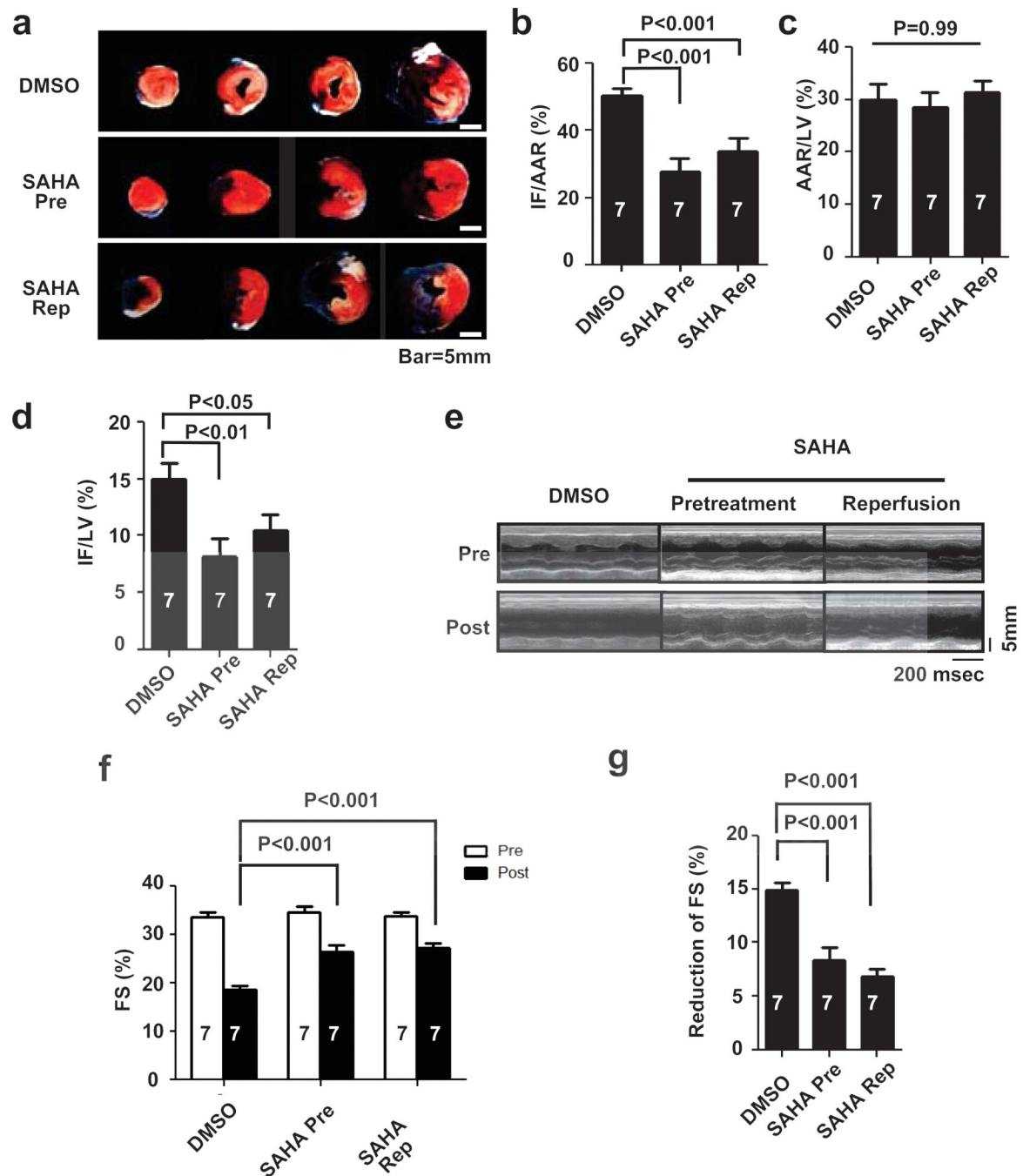


Figure 3. SAHA reduces infarct size and preserves systolic function in a rabbit I/R model. **a.** Representative TTC staining in three treatment groups after I/R (30 min/24 hour). White: Infarct, Red: AAR, Blue: Remote. **b.** SAHA reduced IF/AAR as determined by TTC staining ($n = 7$, $p < 0.001$). **c.** There were no significant differences in AAR among groups. **d.** SAHA reduced IF normalized by left ventricle weight (LV) ($n = 7$, $p < 0.05$). **e.** Representative M-mode echocardiograms. **f.** SAHA treatment partially preserved echocardiography-determined %FS after I/R (30 min/24 hour) ($n=7$, $p < 0.001$). **g.** The reduction in %FS after I/R was significantly lower in the SAHA treatment group ($n=7$, $p < 0.001$).

Rabbit SAHA plasma concentration-time curve (SQ 300mg/kg, n=8)

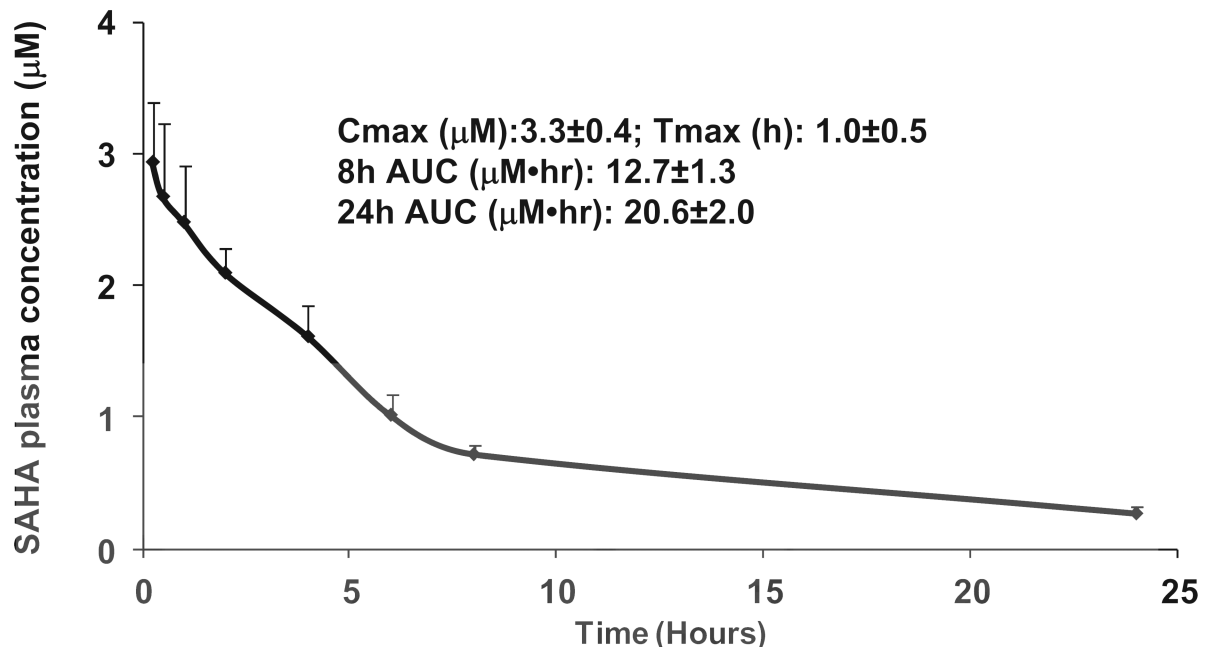
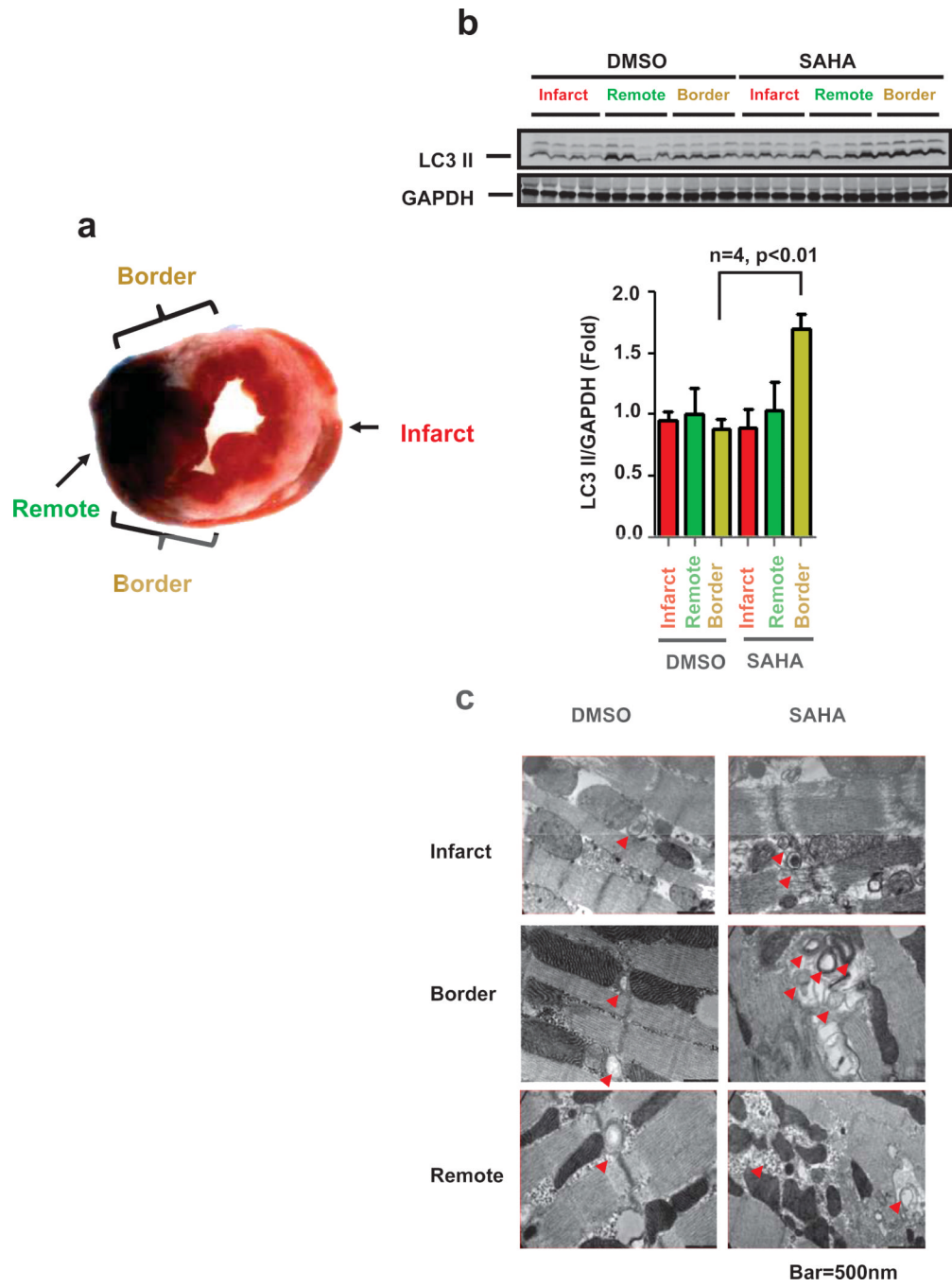


Figure 4. SAHA plasma concentration-time curve in rabbits receiving 300mg/kg at the time of coronary reperfusion. Blood was collected at 15, 30, 60, 120, 240, 360, 480 min and 24 hour after a single dose of SAHA (300 mg/kg SQ) was administered at the time of reperfusion. In eight rabbits, C_{max} was $3.3 \pm 0.4 \mu\text{M}$; T_{max} was 1.0 ± 0.5 hour; 8 hour AUC was $12.7 \pm 1.3 \mu\text{M} \cdot \text{hr}$; 24 hour AUC was $20.6 \pm 2.0 \mu\text{M} \cdot \text{hr}$.



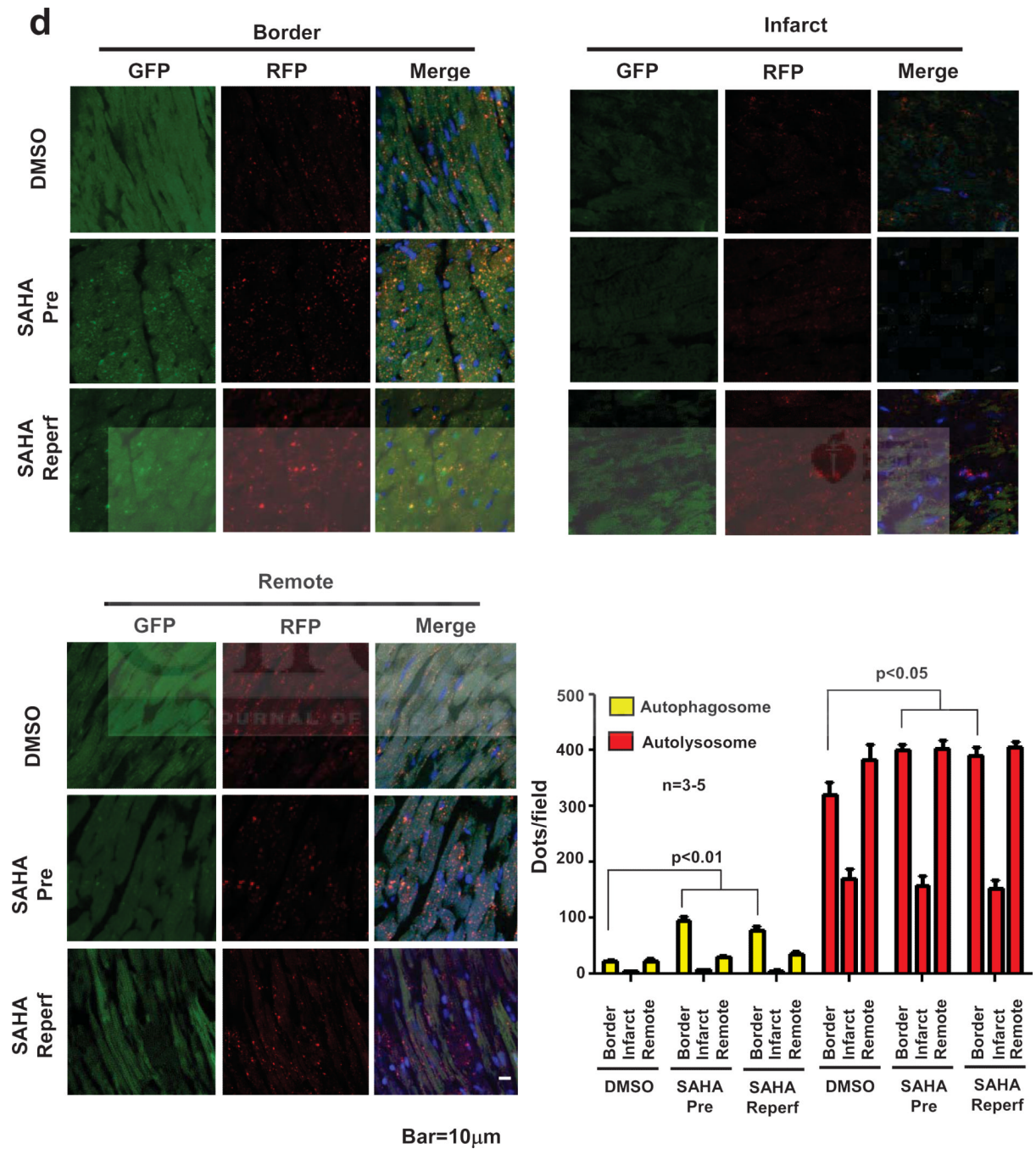


Figure 5. SAHA increases autophagic flux in the infarct border zone. **a.** Rabbit myocardium samples were harvested as depicted for Western blots and EM studies. Red: infarct zone, Green: remote zone, Yellow: border zone. **b. Upper:** LC3 Western blot analysis of protein lysates harvested from the indicated tissue zone (I/R: 30min/2 hour). SAHA was administered only at the time of reperfusion (reperfusion-only group). GAPDH is shown as loading control. **b. Lower:** Quantification. LC3-II normalized to GAPDH. **c.** EM images depicting double membrane autophagosomes. SAHA treatment increased autophagosomes significantly within the border zone (n=3) after I/R (30 min/2 hour). SAHA was administered only at the

time of reperfusion (reperfusion-only group). GAPDH is shown as loading control. **b.** **Lower:** Quantification. LC3-II normalized to GAPDH. **c.** EM images depicting double membrane autophagosomes. SAHA treatment increased autophagosomes significantly within the border zone (n=3) after I/R (30 min/2 hour). **d.** CAG-RFP-GFP-LC3 transgenic mice subjected to I/R (45 min/2 hour). Both yellow dots (autophagosomes) and red dots (autolysosomes) were significantly increased by SAHA treatment within the I/R border zone (n=3-5). Quantification is shown in the right lower panel. Bar=10 μ M.

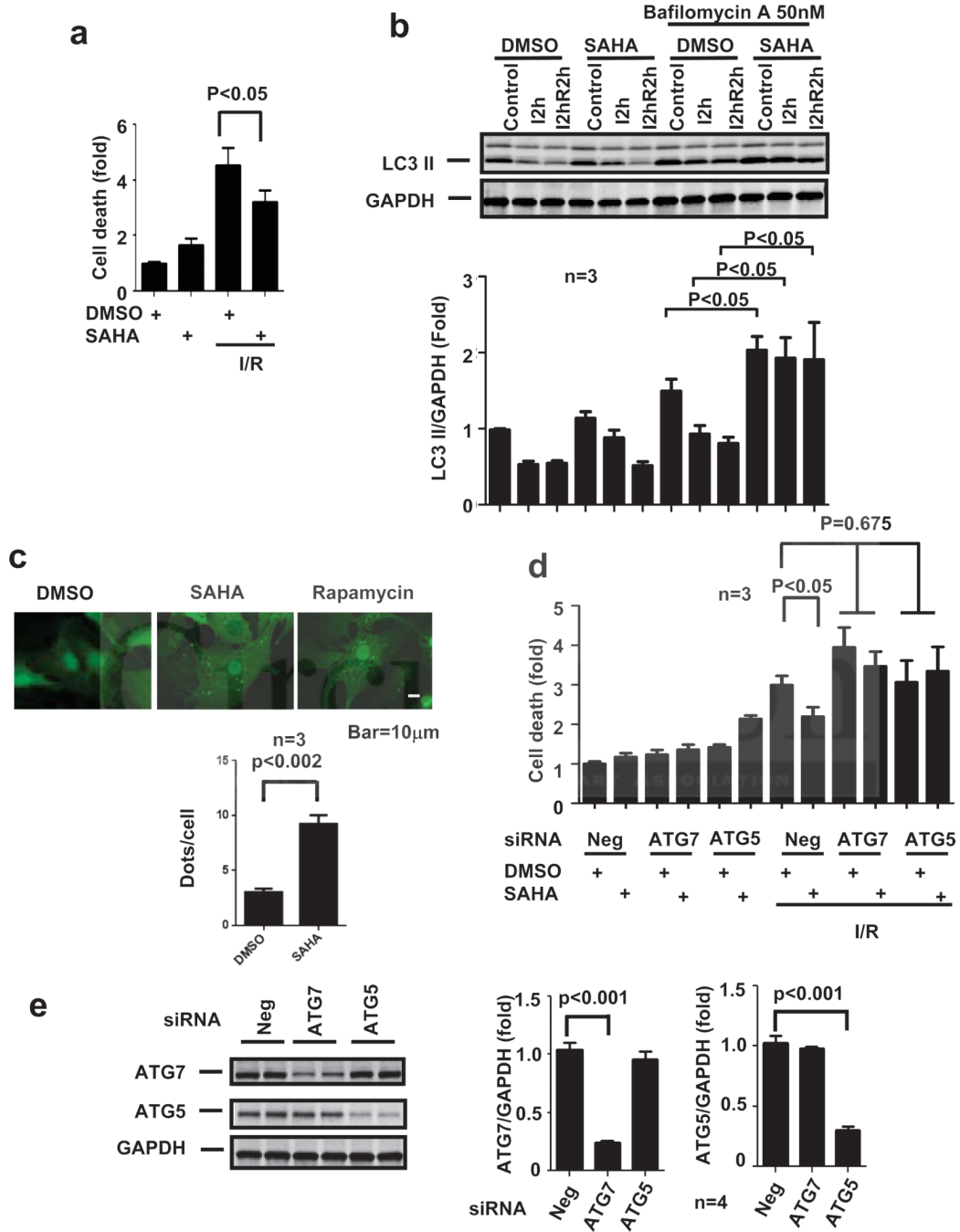


Figure 6. SAHA regulates autophagic flux during I/R, and SAHA's cardioprotective effects are dependent on autophagic flux. **a.** LDH cell death assay. SAHA treatment (2 μ M) reduced cell death around 30% after simulated I/R (sI/R; 5 hour/1.5 hour) (n=3, p<0.05). **b. Upper:** LC3 Western blot. At steady state, LC3-II levels normalized to GAPDH decreased in both DMSO and SAHA groups after 2 hours of ischemia (I2h) and 2 hours of ischemia plus 2 hours of reperfusion (I2hR2h). However, after Bafilomycin A treatment, SAHA treatment induced increases in LC3II levels even after simulated I/R (n=3, p<0.05). **b. Lower:** Quantification. **c.** Autophagic flux measurement using adenovirus hosting GFP-LC3. SAHA

treatment increased autophagic flux as evidenced by increased the GFP-LC3 puncta signal. **d.** LDH cell death assay in the settings of ATG7 or ATG5 knockdown. Suppression of ATG7 and ATG5 both abolished SAHA's cardioprotective effects after sI/R (5 hour/1.5 hour) (n=3, p<0.05). **e.** RNAi knockdown of ATG7 and ATG5. **Left:** Western blots. **Right:** quantification.

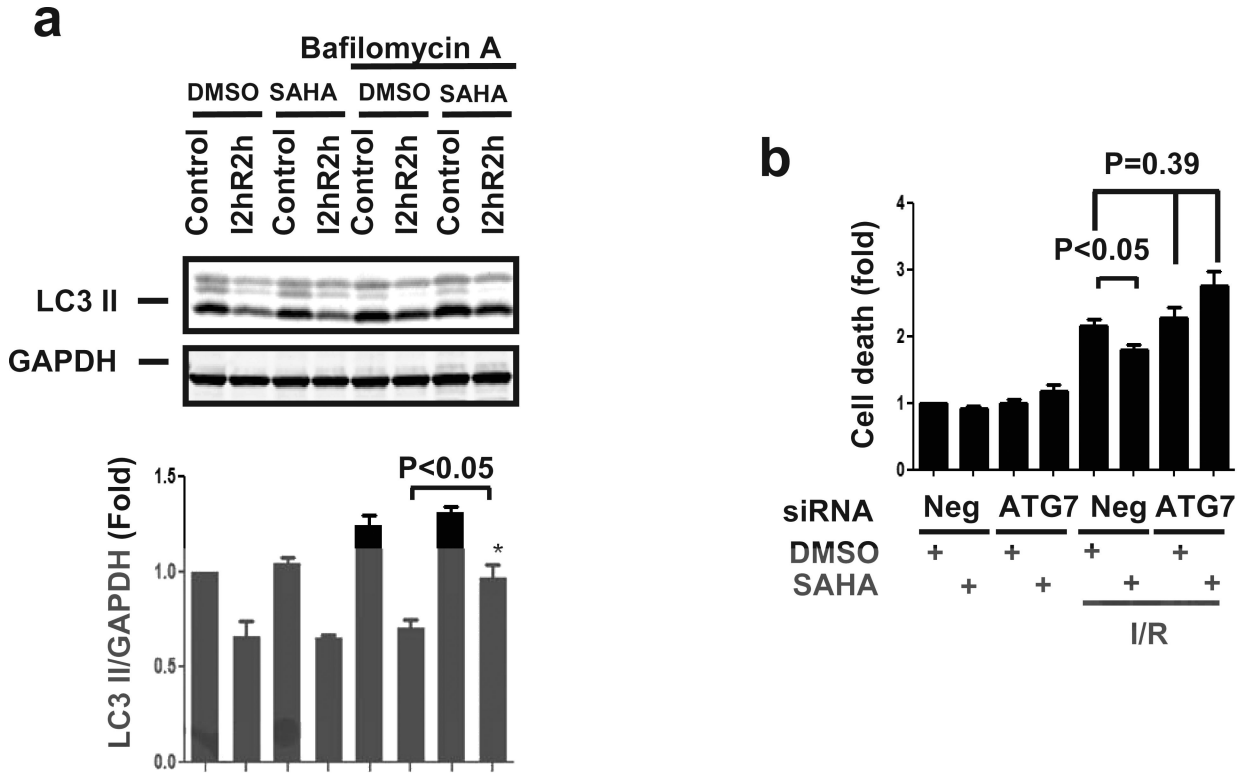


Figure 7.

µa. Upper: LC3 Western blot. At steady state, LC3-II levels normalized to GAPDH decreased in both DMSO and SAHA groups after 2 hours of ischemia plus 2 hours of reperfusion (I2hR2h). However, after Bafilomycin A treatment, SAHA treatment induced increases in LC3II levels after simulated I/R (n=3, p<0.05). **Lower:** Quantification. **b. LDH** cell death assay. SAHA treatment (2µM) reduced cell death around 20% after sI/R (5 hour/ 1.5 hour) (n=3, p<0.05). Suppression of ATG7 abolished SAHA's cardioprotective effects after sI/R (n=3, p<0.05).

Table 1

Comparison of plasma SAHA levels in rabbit with those of human subjects receiving IV SAHA. Measured rabbit plasma SAHA concentration parameters were compared with those from human subjects receiving IV SAHA during a phase 1 clinical trial.

Dose level	n	C _{max} (ng/mL)	AUC _{inf} (h × ng/mL)
300mg/m ²	11	2646 ± 588	4285 ± 1150
300mg/kg SQ rabbit	8	872 ± 106	5438 ± 528
600mg /m ²	9	6334 ± 3086	11233 ± 6928
900mg/m ²	11	9525 ± 1611	16611 ± 4533